Int J Clin Exp Med 2015;8(2):1768-1779
www.ijcem.com /ISSN:1940-5901/IJCEM0003656

Original Article

Protective effect of the traditional Chinese medicine xuesaitong on intestinal ischemia-reperfusion injury in rats

Xuan Xu[1*], Dengxiao Li[2*], Hong Gao[3], Yuejin Gao[4], Long Zhang[5], Yuling Du[1], Jian Wu[6], Pengfei Gao[1]

[1]Department of TCM, Jinshan Hospital Affiliated to Fudan University, Shanghai 201508, China; [2]Department of Rehabilitation, Jinshan Hospital Affiliated to Fudan University, Shanghai 201508, China; [3]Tumor Laboratory, Putuo Hospital, Shanghai University of Traditional Chinese Medicine, Shanghai 200062, China; [4]Animal Room, Putuo Hospital, Shanghai University of Traditional Chinese Medicine, Shanghai 200062, China; [5]Central Laboratory, Putuo Hospital, Shanghai University of Traditional Chinese Medicine, Shanghai 200062, China; [6]Surgical ICU, Putuo Hospital, Shanghai University of Traditional Chinese Medicine, Shanghai 200062, China. [*]Equal contributors.

Received November 6, 2014; Accepted January 21, 2015; Epub February 15, 2015; Published February 28, 2015

Abstract: Objective: We investigated the effect of xuesaitong on intestinal barrier dysfunction and related mechanisms in a rat model for intestinal ischemia-reperfusion. Methods: Rats were divided into sham-operated, disease-model and Xuesaitong-treated groups. In the disease-model and Xuesaitong-treated rats an intestinal ischemia-reperfusion injury (IRI) model was introduced, which was created by a temporary obstruction of the superior mesenteric artery (SMA). The xuesaitong group was pre-treated with injections into the abdominal cavity prior to the generation of the IRI model. Tissue changes were evaluated using H&E staining and electron microscopy. Samples were analyzed at 0, 3 and 24 h post IRI. Ascites volumes as well as small intestinal mucosa bleeding, injury scores, wet to dry weight ratios, and propulsions were evaluated. Apoptotic rates were determined with TUNNEL assays. Blood serum tumor necrosis factor-α (TNF-α) levels were measured using ELISA, and Bcl-2 and caspase-3 expression in small intestinal mucosa measured using immunohistochemistry. Results: We determined a significant increase of pathological damage to small intestinal tissues, intestinal wet to dry ratios, ascites volume, TNF-α levels, apoptosis rates of small intestinal mucosa, and expression of Bcl-2 and caspase-3 proteins in the disease-model group compared to the sham-operated group ($P < 0.001$), and intestinal motility was significantly decreased ($P < 0.001$). However, comparisons between disease-model and xuesaitong pre-treated animals revealed, that in the treatment group these changes occurred in significant less severities. Conclusions: Xuesaitong can effectively alleviate intestinal barrier dysfunction caused by ischemia-reperfusion injury by reducing TNF-α, up-regulating Bcl-2 and down-regulating caspase-3 expression, in addition to increasing peristalsis.

Keywords: Intestinal ischemia-reperfusion, intestinal mucosal barrier function, xuesaitong injections, apoptosis

Introduction

Ischemia-reperfusion injury (IRI) is a common pathological process, which can occur as a treatment complication in many diseases and is a prominent cause of intestinal mucosal barrier dysfunction. Therefore, improvement of intestinal barrier integrity after injury is of great clinical significance for the preservation of bowel functions. Recent studies [1, 2] showed that several conditions, such as severe infection, trauma, shock and severe acute pancreatitis, can cause intestinal ischemia, intestinal barrier dysfunction (IBD), and an increase of intestinal mucosal permeability, which leads to translocation of intestinal bacteria and endotoxins and further stimulation of the reticuloendothelial system, thereby triggering the release of a large number of inflammatory mediators and cytokines. These inflammatory factors can subsequently worsen IBD, which not only causes a “two-hit” injury effect on the intestinal mucosa but also broadly influences the structure and function of remote organs, leading to

Table 1. Small intestinal mucosa bleeding score in each group

	n	Small intestinal mucosa bleeding score				
		0	I	II	III	IV
Sham-operated group	8	6	2	0	0	0
Disease model group 0 min	8	0	0	6	2	0
Disease model group 3 h	8	0	0	0	7	1
Disease model group 24 h	8	0	0	1	6	1
Treatment group 0 min	8	0	6	2	0	0
Treatment group 3 h	8	0	1	7	0	0
Treatment group 24 h	8	0	3	5	0	0

Table 2. Chiu's 6-level scoring for intestinal mucosal injury in each group

	n	Chiu's 6-level scoring for intestinal mucosal injury					
		0	I	II	III	IV	V
Sham-operated group	8	6	2	0	0	0	0
Disease model group 0 min	8	0	0	1	6	1	0
Disease model group 3 h	8	0	0	0	3	5	0
Disease model group 24 h	8	0	0	0	5	3	0
Treatment group 0 min	8	2	5	1	0	0	0
Treatment group 3 h	8	0	4	4	0	0	0
Treatment group 24 h	8	0	5	3	0	0	0

multiple organ dysfunction syndrome (MODS), or even multiple organ failure (MOF). This profound cascade of events can subsequently give rise to IBD, which plays an important role as a prognostic indicator for critically ill patients [1, 2]. Past studies showed correlations of IBD with bowel mucosa hypoperfusion, ischemia-reperfusion of the intestinal mucosa, nutritional disorders, intestinal microflora and endotoxin damage [3]. Recent research on apoptosis in recent years has led to a better understanding of these correlations. However, the mechanisms for the role of apoptosis in IBD and intestinal ischemia-reperfusion remain to be fully elucidated.

A preventative protective approach could potentially avoid pathological processes, which can lead to IBD in surgical patients, but therapeutic strategies for the prevention and repair of the intestinal barrier have yet to be developed. In China, critically ill patients have been treated with a combination of traditional Chinese medicine (TCM) and western medicine in recent years. The TCM differentiation theory attributes microcirculation disorders in early intestinal ischemia-reperfusion to poor blood supply and blood stasis. TCM further describes stagnation and deficiencies in the circulation as causes of pain in patients, and refers to the notogingseng plant, a member of the araliaceae ginseng species, as a remedy to improve the circulation. The plant's active ingredient, panax notoginseng saponins (PNS), was used to develop sterile xuesaitong injections, which are widely used prior to clinical procedures. Recent research studies [4, 5] suggested that PNS acts as an antioxidant, can regulate cellular factors, expands blood vessels, improves microcirculation, reduces apoptosis and plays a protective role during vital organ damage involving liver, lung, kidney, brain, spinal cord and muscles. However, no such studies exist on a potential protective effect of xuesaitong on intestinal barrier function.

Prophylactic pretreatment through ischemic preconditioning has been described in previous studies [6]. Our study uses a rat model for intestinal ischemia-reperfusion to investigate the effectiveness of xuesaitong injections for preventive IBD medication.

Experimental materials and methods

Experimental animals and pre-treatment

56 clean grade healthy male SD (Sprague-Dawley) rats were provided by the Sino-British joint venture Shanghai experimental animal Co. LTD. Animals weighed 200~250 g, were 6-8 weeks of age, and were kept under standard conditions with access to food and water ad libitum. Experiments were conducted after adaptive feeding for 7 days. All animal experiments were done according the regulation of animal experiments published by the Chinese state council.

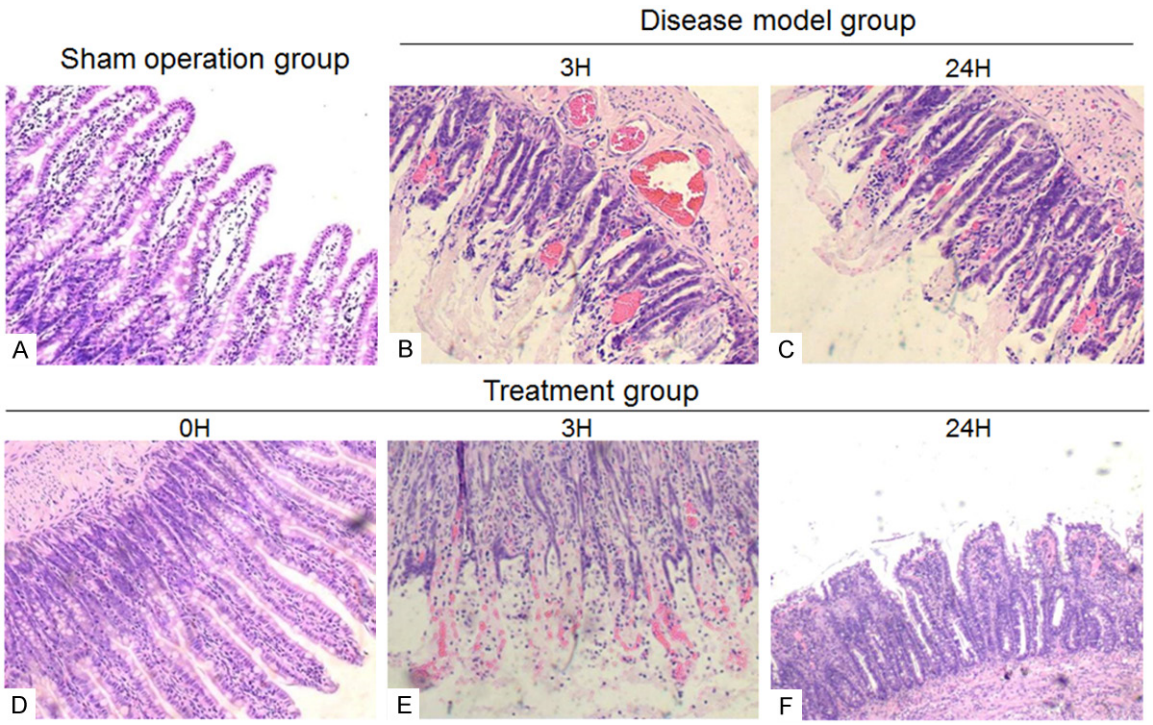

Figure 1. H&E staining in intestinal tissue (A) sham-operated group (B, C) disease-model group (D-F) treatment group.

Animal disease model and experimental design

Experimental animals were randomly divided into 3 groups, a sham-operated group, a disease-model group, and a xuesaitong-treated group. An intestinal ischemia-reperfusion injury (IRI) model was created by obstructing the superior mesenteric artery (SMA) for 60 minutes and then restoring blood flow. The rats were starved for 12 h with access to water, and were abdominally injected with 2.5% pentobarbital sodium (50 mg/kg) prior to surgery. Through a midline incision in the upper abdomen, the SMA was located, dissociated, and compressed at the proximal end with an artery clamp. Obstruction was confirmed by a color change in the small intestinal wall and a weakening of the SMA pulse. During surgery, all animals were abdominally injected with saline solutions to maintain hemodynamic stability, and any animals that died during the procedure were excluded and supplemented. Gastric tissue was perfused with a carbon powder suspension 1 h prior to sacrifice. Sampling was done at 0 min, 3 h and 24 h after reperfusion (8 samples in each group). Because in the sham-operated group the SMA was not obstructed this group served for control data and was sacrificed only at the 24 h time point.

Drug administration

Xuesaitong injection solution was provided from the Putuo Hospital affiliated to the Shanghai Traditional Chinese Medicine University. The main ingredient was 250 mg saponins of panax notoginseng (PNS) per 5 ml saline (Kunming Pharmaceutical Group Co. Ltd.; approval number Z53020665).

In the treatment group, animals were abdominally injected with 6.58 mg/kg qd xuesaitong 1 week prior to creation of the disease model, and animals in the sham-operated and disease-model group were abdominally injected with saline solution in the same manner and dose. Xuesaitong injection dosage was calculated using the formula $dB = dA \times RB/RA \times (WA/WB)^{1/3}$, where dA and dB designate the dose per kilogram of body weight in human and rats, respectively (in mg/kg); RA and RB designate shape coefficients of human and rats, respectively (RA = 100, RB = 59); WA and WB designate weight values of humans and rats,

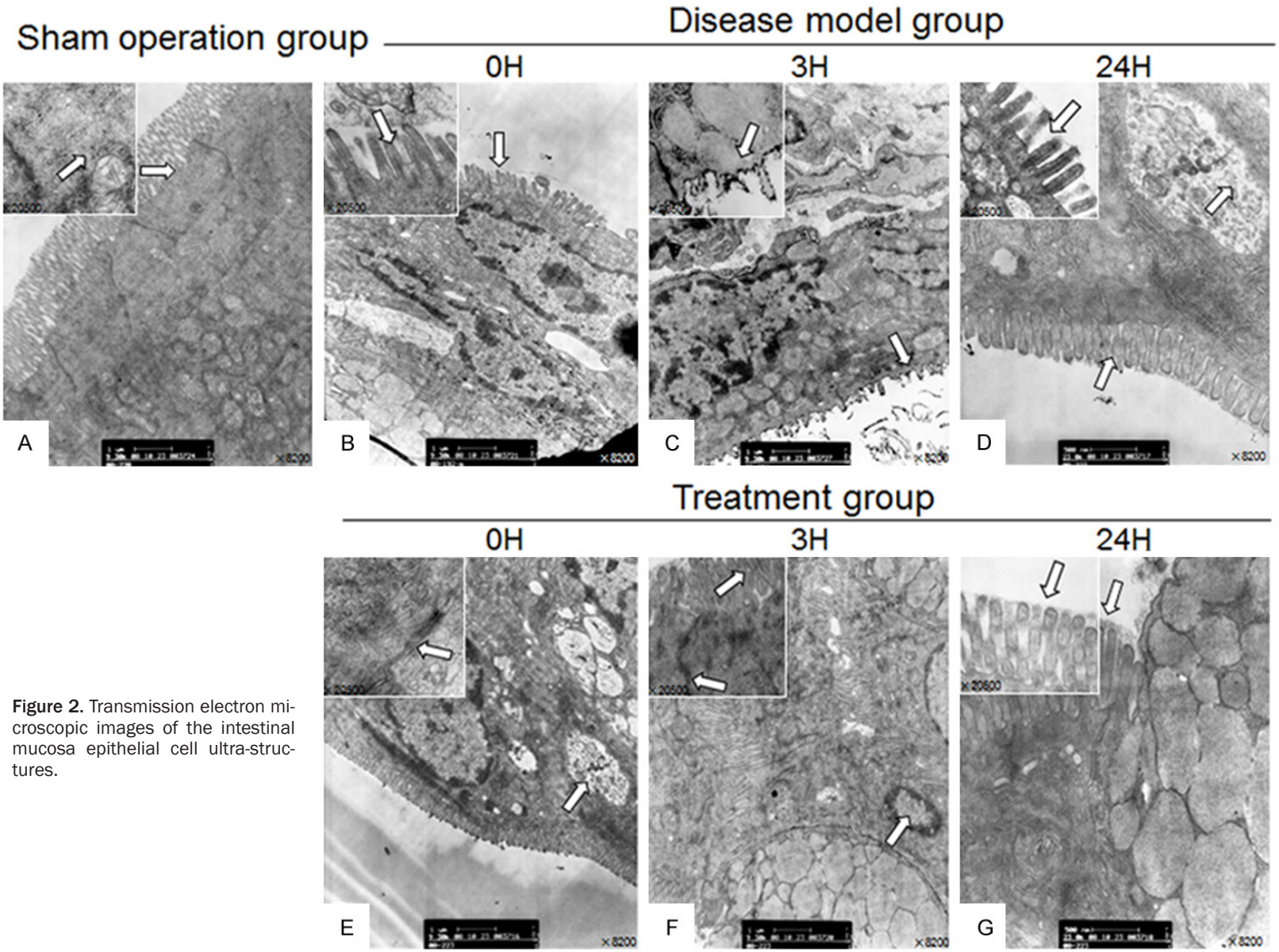

Figure 2. Transmission electron microscopic images of the intestinal mucosa epithelial cell ultra-structures.

Table 3. Small intestine tissue wet to dry weight ratio in each group

Group	n	Small intestine tissue wet to dry weight ratio ($\bar{x}$ ± SD)		
Sham operated group	8	3.87 ± 0.12		
		0 min	3 h	24 h
Disease model group	8	4.20 ± 0.16$^{▲▲▲}$	6.42 ± 0.24$^{▲▲▲}$	4.51 ± 0.23$^{▲▲▲}$
Treatment group	8	3.93 ± 0.07$^{Δ,◆◆◆}$	4.38 ± 0.22$^{ΔΔΔ,◆◆◆}$	4.22 ± 0.20^{Δ}

Sham vs Disease $^{▲▲▲}P < 0.001$; Sham vs Treatment $^{Δ}P < 0.05$, $^{ΔΔΔ}P < 0.001$; Disease vs Treatment $^{◆◆◆}P < 0.001$.

Table 4. Ascites volume in each group

Group	n	Ascites volume (mL, $\bar{x}$ ± SD)		
Sham operated group	8	0.19 ± 0.08		
		0 min	3 h	24 h
Disease model group	8	0.48 ± 0.10$^{▲▲▲}$	1.15 ± 0.12$^{▲▲▲}$	0.99 ± 0.08$^{▲▲▲}$
Treatment group	8	0.30 ± 0.08$^{Δ,◆◆}$	0.46 ± 0.05$^{ΔΔΔ,◆◆◆}$	0.43 ± 0.07$^{ΔΔΔ,◆◆◆}$

Sham vs Disease $^{▲▲▲}P < 0.001$; Sham vs Treatment $^{Δ}P < 0.05$, $^{ΔΔΔ}P < 0.001$; Disease vs Treatment $^{◆◆}P < 0.01$, $^{◆◆◆}P < 0.001$.

Table 5. Small intestinal propulsion rate

	n	Small intestinal propulsion rate (%, $\bar{x}$ ± SD)		
Sham operated group	8	61.34 ± 0.59		
		0 min	3 h	24 h
Disease model group	8	56.56 ± 0.59$^{▲▲▲}$	51.60 ± 0.90$^{▲▲▲}$	52.17 ± 0.64$^{▲▲▲}$
Treatment group	8	61.24 ± 1.01$^{◆◆◆}$	60.52 ± 0.78$^{Δ,◆◆◆}$	60.77 ± 0.42$^{Δ,◆◆◆}$

Sham vs Disease $^{▲▲▲}P < 0.001$; Sham vs Treatment $^{Δ}P < 0.05$; Disease vs Treatment $^{◆◆◆}P < 0.001$.

Table 6. Apoptotic rate of intestinal mucosal epithelial cells in each group

Group	n	Apoptotic rate of intestinal mucosal epithelial cells (%, $\bar{x}$ ± SD)		
Sham operated group	8	22.46 ± 4.09		
		0 min	3 h	24 h
Disease model group	8	28.78 ± 1.17$^{▲▲▲}$	51.75 ± 7.73$^{▲▲▲}$	29.22 ± 1.64$^{▲▲▲}$
Treatment group	8	22.82 ± 1.43$^{◆◆◆}$	26.30 ± 3.21$^{Δ,◆◆◆}$	22.67 ± 2.12$^{◆◆◆}$

Sham vs Disease $^{▲▲▲}P < 0.001$; Sham vs Treatment $^{Δ}P < 0.05$; Disease vs Treatment $^{◆◆◆}P < 0.001$.

respectively (60 kg vs. 200 g as the standard body weight of human and rats).

Observational indicators and measurement techniques

Bleeding degree of small intestinal mucosa: The bleeding degree of the small intestinal mucosa was scored according to Nackel's rating method: 0 for no bleeding, 1 for scattered punctate bleeding, 2 for bleeding which accounted for a quarter of the intestinal segment; 3 for bleeding which accounted for 50% of the intestinal segment; 4 for bleeding in almost all of the small intestine.

Histology

Ileum tissue was fixed with cold 2.5% glutaraldehyde (pH 7.4), rinsed with PBS, fixed in cold 1% osmic acid, washed with PBS, kept in saturated uranium acetate, dehydrated with acetone, treated with epoxy propane, and embedded in saturated epoxy resin 618. Ultrathin tissue slices were produced using a microtome and any changes in intestinal tissue ultrastructure detected by transmission electron microscopy. Small intestinal tissue samples were fixed in 10% (3.33 mmol/L) neutral formaldehyde, dehydrated, paraffin embedded, and sliced into 2-3 μm thick sections for H&E staining. Damage to the small intestinal mucosa was scored according to Chiu's 6-level scoring method for intestinal mucosal damage after inspection of sections with a light microscope [7].

Measurement of wet to dry weight ratios and ascites volumes in intestinal tissue

Intestinal tissues were quantitatively removed and weighed to determine the wet weight (W), while dry weight (D) was determined after drying the tissues in a 56°C constant temperature box for 24 h. The wet to dry weight ratio (W/D)

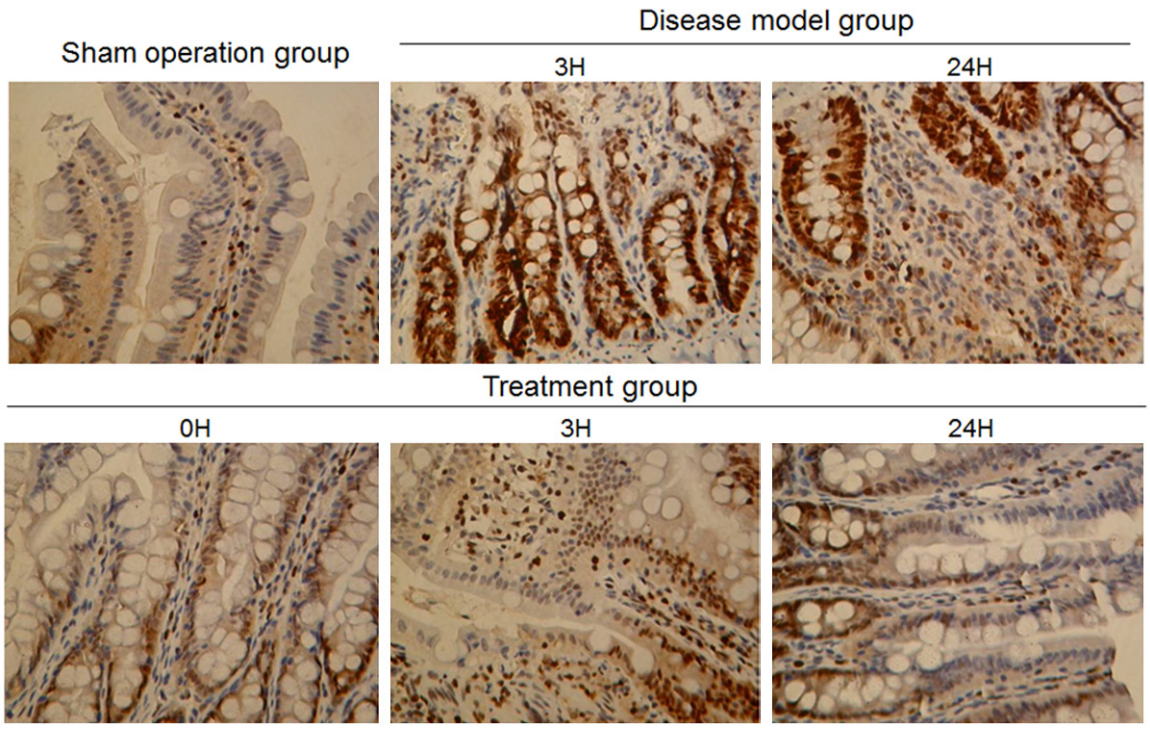

Figure 3. Representative images of TUNEL staining of epithelial cells in the intestinal mucosa (Magnification × 400).

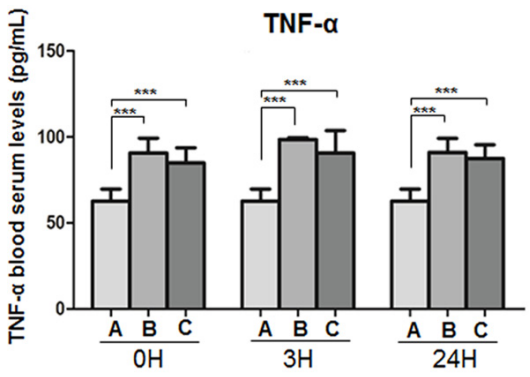

Figure 4. TNF-α blood serum concentrations in (A) the sham operated, (B) the disease model and (C) the treatment animals at the indicated time points. ***$P < 0.01$.

was then calculated. All ascites liquids were extracted from the abdomen and the amounts were recorded.

Measurement of small intestinal propulsion rate

The small intestinal propulsion rate was calculated using an activated powdered carbon labeling method. Rats were sacrificed 1 h after perfusion with 4.5 mL of an activated carbon suspension. The abdomen was opened, the intestinal canal removed, and the length of pigment propulsion and the total length of the small intestine measured. The percentage between them was recorded as the small intestinal propulsion rate and used to estimate intestinal peristalsis. The propulsion rate was calculated using the following formula: % propulsion rate of carbon powder = propulsive length of carbon powder (cm)/total length of small intestine (cm) × 100%.

Apoptosis and ultrastructure of intestinal mucosal epithelial cells

Apoptosis of small intestinal mucosal epithelial cells was determined using the TUNEL *in situ* detection kit (Nanjing KeyGen Biotech. Co. Ltd, Nanjing, China) following the manufacturer's instructions. 100 cells were counted in each of 10 randomly selected fields and the percentage of positive cells was determined using the formula: percentage of positive cells = positive cell number/total cell count × 100%. The ultrastructure of the intestinal mucosal epithelial cells was analyzed using an electron microscope.

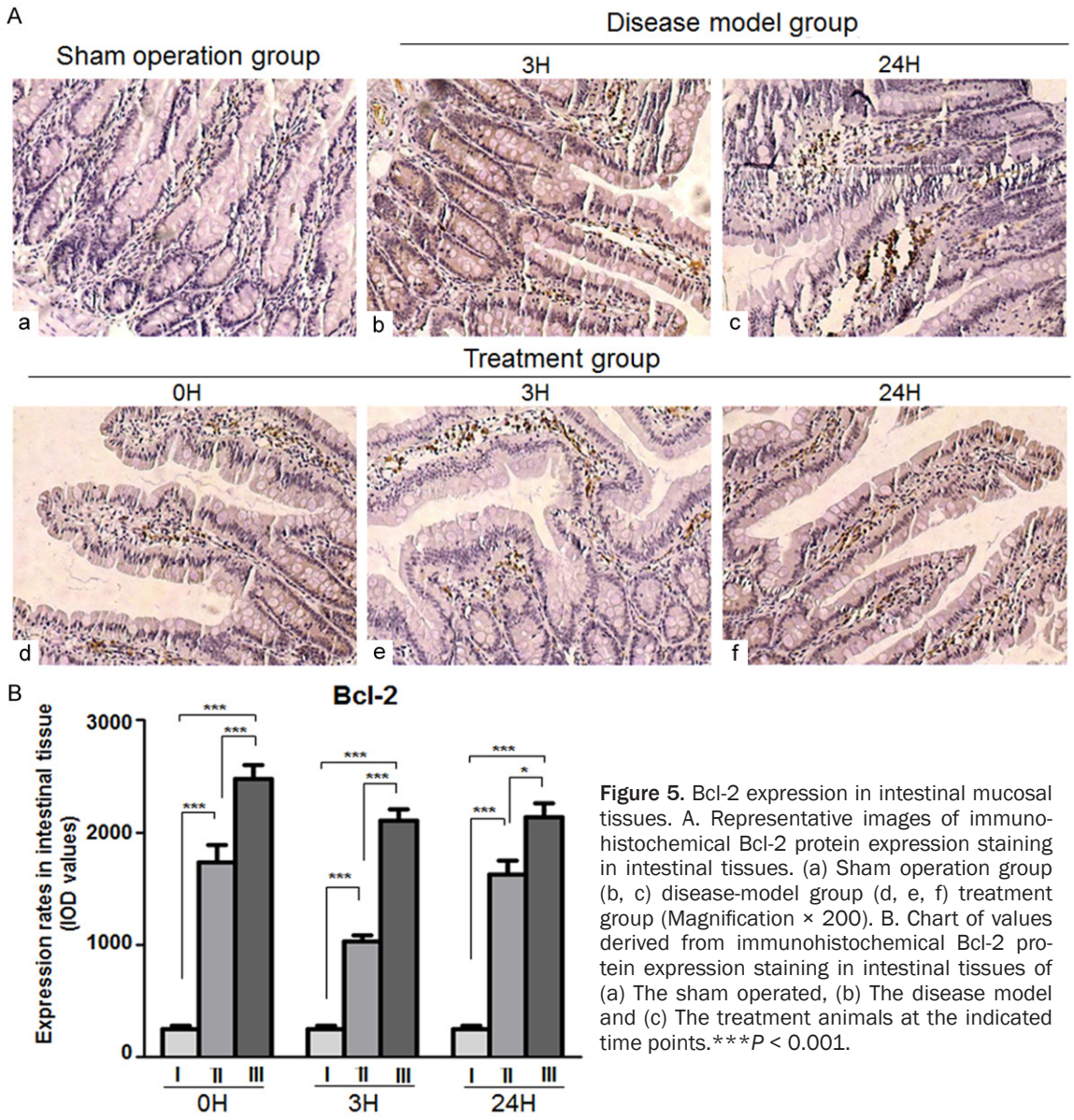

Figure 5. Bcl-2 expression in intestinal mucosal tissues. A. Representative images of immunohistochemical Bcl-2 protein expression staining in intestinal tissues. (a) Sham operation group (b, c) disease-model group (d, e, f) treatment group (Magnification × 200). B. Chart of values derived from immunohistochemical Bcl-2 protein expression staining in intestinal tissues of (a) The sham operated, (b) The disease model and (c) The treatment animals at the indicated time points.***$P < 0.001$.

Bcl-2 and caspase-3 quantification

Expression of Bcl-2 and caspase-3 proteins was detected using immunohistochemistry. Small intestinal tissue was fixed in formaldehyde, paraffin embedded, and analyzed using the rabbit anti-rat Bcl-2 polyclonal antibody and rabbit anti-rat caspase-3 polyclonal antibody kit (CHEMICON Company, USA). The immunohistochemical staining was quantified using Image-Pro Plus 5.0 fully automated image analysis software (Media Cybernetics, USA). Six sections were randomly selected from each group, and 3 fields were selected in each section at × 200 magnification, with an integral optical density (IOD) value of 3 fields as the final output.

Measurement of serum TNF-α levels

Blood serum TNF-α levels were measured using an enzyme-linked immunosorbent assay (ELISA) (Rat TNF alpha ELISA detection kit, Rapidbio) according to the manufacturer's instructions. Blood samples were taken from the abdominal aorta.

Statistical analyses

All statistical analyses were calculated using SPSS for Windows (Version 16.0, Chicago,

SPSS Inc). Experimental data are presented as the $\bar{x} \pm SD$ (except for the small intestinal mucosa bleeding degree and Chiu scoring). Comparison of multiple sample means was done with one-way ANOVA. The mean differences between groups were first tested for homogeneity of variance and then compared with the least significant difference (LSD) or Fisher LSD if the variance was homogeneous or with the Game Howell method if the variance was heterogeneous. The multiple sample comparisons of small intestinal mucosa bleeding degree and Chiu scoring were calculated with a Kruskal-Wallis H test. The difference was regarded as significant if $P < 0.05$.

Results

Xuesaitong injections reduce damage to the intestinal mucosa in an intestinal ischemia-reperfusion rat model

Rats in the disease-model group were characterized by severe intestinal congestion, with parts of the intestinal canal showing purple discolorations, which were most severe at 3 h of reperfusion. However, a comparison at the same time point in the xuesaitong group revealed a much milder degree of congestion, with some intestinal diffuse bleeding and hemorrhage and no obvious differences between the time points studied. Intestinal congestion could barely be observed in the sham-operated group. The scoring results for small intestinal mucosal bleeding are summarized in **Table 1**. We found that the degree of small intestinal mucosal hemorrhage in the disease-model group was mostly level-II (6/8, 75%), small intestinal mucosal hemorrhage predominantly in level-III (7/8, 87.5%) at 3 h of reperfusion, and small intestinal mucosal bleeding at level-III 75% (6/8) after 24 h. After treatment, small intestinal mucosal bleeding at level-III was minimal and improved after 3 h of treatment to 87.5% at level-II (**Table 1**).

Based on Chiu's 6-level scoring, 75% of intestinal mucosal injury was assessed at level-II, while 25% was at level-III. After 3 h of reperfusion, 87.5% of mucosal injury was at level-III, while 12.5% was at level-IV, and at 24 h reperfusion 75% of injury to the mucosa was at level-III, while 12.5% was at level-II and level-IV. However, all of these values were improved after xuesaitong treatment, with a shift towards level-I or level-II (**Table 2**).

Observation of pathological morphology in small intestinal tissue and Chiu's 6-level scoring for damage to the intestinal mucosa

H&E staining in the sham-operated group revealed an intact structure of the intestinal mucosa, neatly aligned villi, tightly connected intestinal epithelial cells, an intact mechanical barrier, no infiltration of inflammatory cells into the mucosa and submucosa, compact arrangement of the lamina propria, and no bleeding or ulceration (**Figure 1A**). Conversely, the disease-model group was characterized by serious intestinal mucosal injury, short and thin villi, wider villi spacing, necrosis and collapse of intestinal mucosal epithelial cells, infiltration by inflammatory cells, gap formation beneath the epithelium, lamina propria edema, and extensive capillary hemorrhage at different reperfusion times (**Figure 1B**, **1C**). The 3 h sampling lesions were more severe than the 0 h and 24 h lesions at the different reperfusion times. However, a comparison of the corresponding reperfusion times between the disease-model and the xuesaitong-treated rats revealed a healthier formation of the intestinal mucosa, and short and thin small intestinal villi. Neutrophil infiltration in the intestinal mucosa was negligible, the expansion of the central lacteals was mild and the intestinal mucosa was relatively complete. There were a few collapsed intestinal epithelial cells and mild hyperemia as well as edema under the epithelial cells after treatment was detected (**Figure 1D-F**).

Transmission electron microscopy analysis of the intestinal mucosal cell ultrastructure

Analysis by transmission electron microscopy revealed that the sham-operated group was characterized by an intact cell structure of the intestinal mucosal epithelium, which was complete and neatly arranged, with clear tight junctions between epithelial cells, intact organelles, and the cytoplasm contained a large number of mitochondria with integer structure and a clear crest (**Figure 2A**). In the disease-model group, the microvilli of intestinal mucosal epithelial cells were sparse, shorter and irregularly arranged. The previously tight junctions between epithelial cells appeared fuzzy or damaged, with widened intercellular spaces. Some

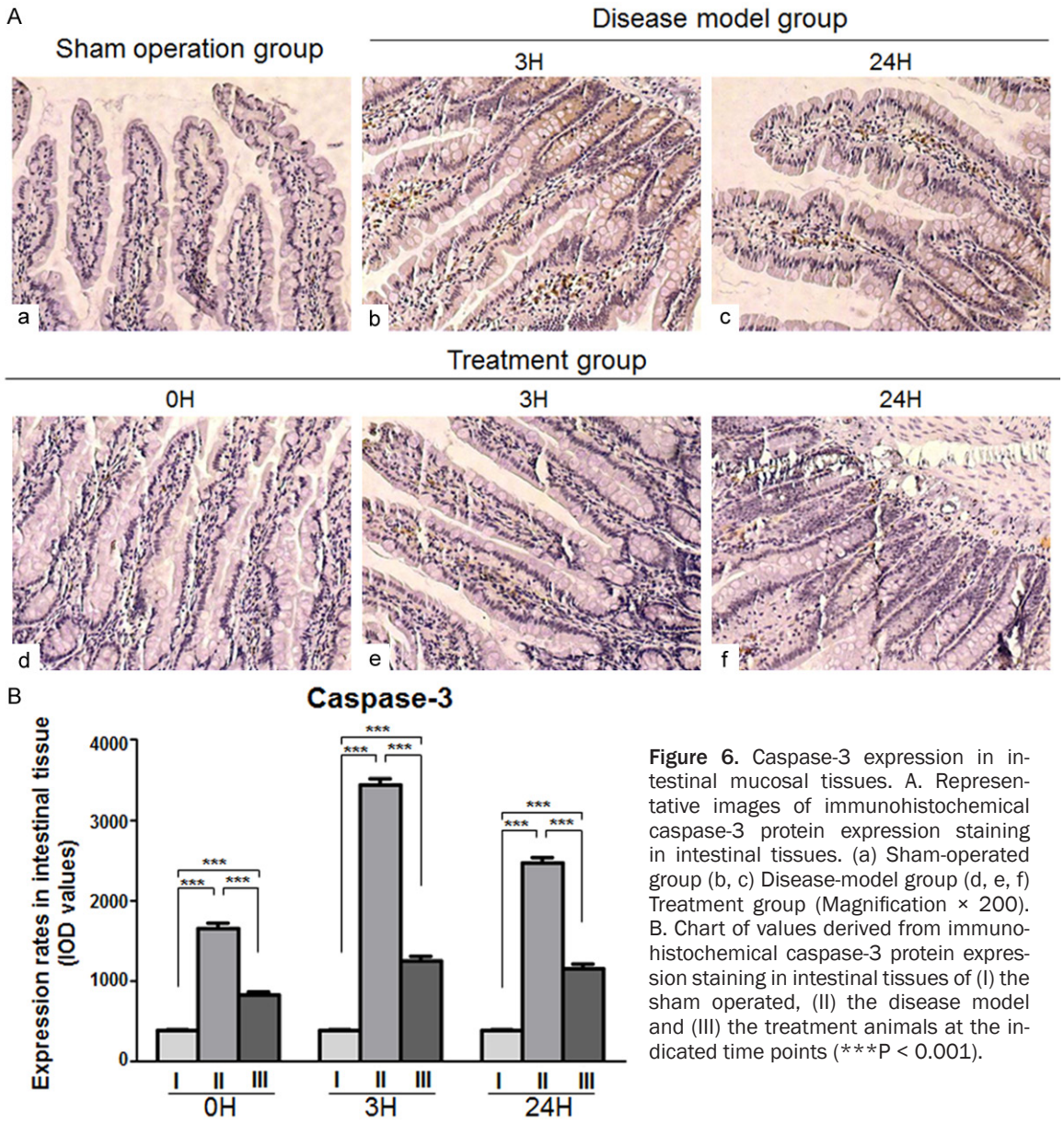

Figure 6. Caspase-3 expression in intestinal mucosal tissues. A. Representative images of immunohistochemical caspase-3 protein expression staining in intestinal tissues. (a) Sham-operated group (b, c) Disease-model group (d, e, f) Treatment group (Magnification × 200). B. Chart of values derived from immunohistochemical caspase-3 protein expression staining in intestinal tissues of (I) the sham operated, (II) the disease model and (III) the treatment animals at the indicated time points (***P < 0.001).

mitochondria appeared swollen, with a dissolved crest and degeneration of vacuoles. The endoplasmic reticulum looked disordered, and a number of nuclei appeared pyknotic, with an uneven membrane surface displaying the morphological changes associated with apoptosis. The second phase lesions (**Figure 2C**) were more severe than the first (**Figure 2B**) and third phase lesions (**Figure 2D**). In the treatment group, microvilli of intestinal mucosal epithelial cells were slightly shorter, neatly arranged and large areas of necrosis were absent. The tight junctions between epithelial cells were orderly. Mitochondria did not show any obvious cavity or crest deformations and overall the swelling in the endoplasmic reticulum was mild (**Figure 2E**, **2F**).

Xuesaitong reduced intestinal tissue edema and ascites formation and improved intestinal peristalsis in intestinal ischemia-reperfusion rats

The intestinal tissue wet to dry weight ratios at different perfusion times in the disease-model group were significantly higher than those in the sham-operated group ($P < 0.001$), suggesting that intestinal ischemia-reperfusion caused

profound tissue edema, which was especially severe at the second and third time points. The wet to dry weight ratio in the treatment group was significantly lower compared to the values of the corresponding time points for the disease-model group at 0 h and 3 h ($P < 0.001$) and the differences between the sham-operated and treatment group ($P < 0.05$) was less than the difference for the disease model and sham operated groups ($P < 0.001$), suggesting that xuesaitong injections could lower the degree of intestinal tissue edema (**Table 3**).

The ascites volumes at different time points in the disease-model group were significantly higher than those in the sham-operated group ($P < 0.001$), and the ascites volumes in the second phase were higher than in the first and third phases in the disease-model group. Ascites volumes in the treatment group were significantly lower compared to the corresponding time points in the disease-model (**Table 4**).

The intestinal peristalsis rate in experimental animals decreased after intestinal ischemia reperfusion and the values were significantly lower at each time point in the disease-model group compared to the sham-operated group ($P < 0.001$). Conversely, the intestinal peristalsis rates were significantly higher in the treatment group compared to the corresponding time points in the disease-model group ($P < 0.001$, **Table 5**).

Xuesaitong led to reductions of serum TNF-α levels and intestinal mucosal epithelial cell apoptosis in ischemia-reperfusion rats, up-regulation of the anti apoptotic Bcl-2 protein, as well as downregulation of the pro-apoptotic protein caspase-3

The apoptotic rate of the intestinal mucosa was significantly higher at each time point in the disease-model group than in the sham-operated group ($P < 0.001$). The apoptotic rate in the second phase was significantly higher than that in the first and third reperfusion phase ($P < 0.01$). Apoptosis was lower in the treatment group compared to the disease-model group at all corresponding time points ($P < 0.001$). No significant differences in intestinal mucosal apoptosis were found between treatment and sham-operated group, with the exception of the second reperfusion phase ($P > 0.05$, **Table 6**; **Figure 3**).

Serum TNF-α levels at each time point were significantly higher in the disease-model and treatment groups compared to the sham-operated group ($P < 0.001$). There was a trend for serum TNF-α levels to be lower in the treatment group compared to the corresponding time points in the disease-model but statistical significance was not reached (**Figure 4**).

Bcl-2 protein expression was only weak in the intestinal mucosal tissue of the sham-operated group. Bcl-2 levels were significantly higher in the disease-model group at each time point compared to the sham-operated group ($P < 0.001$). Furthermore, Bcl-2 expression levels were increased after xuesaitong treatment at all corresponding time points and showed significant differences compared to the disease-model group ($P < 0.001$, **Figure 5**).

The level of expressed caspase-3 was significantly higher in the intestinal mucosal tissue of the disease model and treatment group compared to the sham operated animals ($P < 0.001$), but it is noteworthy that the expression level after treatment was far lower than without treatment ($P < 0.001$, **Figure 6**).

Discussion

The incidence of intestinal ischemia-reperfusion injury is relative high in the clinic and a major contributor to intestinal mucosal barrier dysfunction; a high metabolism, and a complex villi capillary structure, makes intestinal mucous membranes extremely sensitive to insufficient blood flow [8, 9]. Under normal conditions, 30% of the circulating blood flows through the gastrointestinal tract [10-13], but under ischemic conditions, low perfusion and severe gastrointestinal hypoxia occurs, leading to deficiencies in mitochondrial respiration and increased glycolysis, exhaustion of cellular ATP, intracellular acidosis and mucosal cell damage, which eventually results in intestinal barrier dysfunction and translocation of endotoxins and bacteria [12, 14, 15].

TNF-α has been reported to trigger epithelial barrier dysfunction by triggering apoptosis [16]. Consistent with the results of Jiang [17], we found that TNF-α levels in peripheral blood were significantly increased after intestinal ischemia reperfusion and reached peak levels 3 h after reperfusion, decreased at 24 h, but

remained significantly increased compared to the early time points of reperfusion ($P < 0.001$).

We suggest that one of the major causes of intestinal dysfunction after clamping of the superior mesenteric artery is abnormal apoptosis of intestinal epithelial cells due to ischemic hypoxia. Xuesaitong injections attenuate apoptosis in the intestinal mucosa and thus protect its normal physiological function by upregulating the expression of the anti-apoptotic Bcl-2 protein and by downregulating the expression of the pro-apoptotic caspase-3 protein in damaged cells, which occurs to a larger extent during the early stages of reperfusion (**Figures 4**, **5**).

Mesenteric vascular hypoperfusion can lead to ischemia of the gastrointestinal mucosa, hypoxia and an increase in vascular permeability. When occurring in capillaries, this can result in mucosal epithelial edema, interstitial edema, or even intraperitoneal fluid accumulation. Capillary permeability in the intestinal canal would be further increased after ischemia reperfusion. We analyzed wet to dry weight ratios in the small intestine as well as ascites volumes to assess indirectly capillary permeability in intestinal tissue. The results showed significant increases at each time point in the disease-model group compared to sham-operated animals, suggesting the occurrence of intestinal capillary leakage. This appeared to be ameliorated after xuesaitong pre-treatment, indicating that this compound can significantly improve the function of the microcirculation, lower capillary permeability and reduce inflammatory edema of the intestinal canal. These actions prevent the intestinal injury that occurs as a result of a vicious circle of circulatory blood volume decrease and intestinal hypoperfusion.

TCM has previously demonstrated the effects of notoginseng on the promotion of blood circulation and the amelioration of blood stagnation. The plant's active ingredient, panax notoginseng saponins (PNS), is formulated in xuesaitong injections, and its main pharmacological effects include: (1) endothelin receptor antagonistic effects, expanding capillaries and increasing blood flow through changes in nitric oxide/nitric oxide synthase signaling pathways [18]; (2) reduction of blood viscosity [19]; (3) reduction of O_2 consumption, increased resistance to free radicals and calcium overload [20]; (4) prevention of an increase in brain cell and vascular membrane permeability caused by ischemia, as well as cytotoxic edema of brain cells caused by sodium retention [5]; (5) induction of platelet secretions such as degranulation to trigger hemostatic and coagulatory events.

In summary, we have demonstrated that intestinal mucosal ischemia-reperfusion causes damage to the structure of the intestinal mucosa, intestinal capillary leakage, and lowered intestinal peristalsis. Our study has shown that mucosa injuries caused by IRI can effectively be diminished by the prophylactic application of xuesaitong. This treatment produced an increase in peristalsis, upregulation of Bcl-2 and downregulation of caspase-3, with concomitantly less apoptotic rates of intestinal mucosal tissue after reperfusion in the IRI rat model. However, additional studies on the beneficial effects of the compound as a clinical pretreatment strategy will be necessary.

Acknowledgements

The study was funded by the Putuo Hospital affiliated to the Shanghai traditional Chinese Medicine University and Natural Science Foundation of China (81473610).

Disclosure of conflict of interest

None.

Address correspondence to: Pengfei Gao, Department of TCM, Jinshan Hospital Affiliated to Fudan University, No. 1508, Longhang Road, Shanghai 201508, China. Tel: +86-18930819385; Fax: +86-021-67226910; E-mail: gaopengfeibm@163.com

References

[1] Acosta S. Epidemiology of mesenteric vascular disease: clinical implications. Semin Vasc Surg 2010; 23: 4-8.

[2] Ahmad ST, Arjumand W, Nafees S, Seth A, Ali N, Rashid S and Sultana S. Hesperidin alleviates acetaminophen induced toxicity in Wistar rats by abrogation of oxidative stress, apoptosis and inflammation. Toxicol Lett 2012; 208: 149-161.

[3] Fink MP and Delude RL. Epithelial barrier dysfunction: a unifying theme to explain the pathogenesis of multiple organ dysfunction at

the cellular level. Crit Care Clin 2005; 21: 177-196.
[4] Zhang HS and Wang SQ. Notoginsenoside R1 inhibits TNF-alpha-induced fibronectin production in smooth muscle cells via the ROS/ERK pathway. Free Radic Biol Med 2006; 40: 1664-1674.
[5] Zhang WJ, Wojta J and Binder BR. Notoginsenoside R1 counteracts endotoxin-induced activation of endothelial cells in vitro and endotoxin-induced lethality in mice in vivo. Arterioscler Thromb Vasc Biol 1997; 17: 465-474.
[6] Son JY, Chandler B, Feketova E, Qin Y, Quackenbush EJ and Deitch EA. Oral pretreatment with recombinant human lactoferrin limits trauma-hemorrhagic shock-induced gut injury and the biological activity of mesenteric lymph. J Surg Res 2014; 187: 270-277.
[7] Chiu CJ, McArdle AH, Brown R, Scott HJ and Gurd FN. Intestinal mucosal lesion in low-flow states. I. A morphological, hemodynamic, and metabolic reappraisal. Arch Surg 1970; 101: 478-483.
[8] Cerqueira NF, Hussni CA and Yoshida WB. Pathophysiology of mesenteric ischemia/reperfusion: a review. Acta Cir Bras 2005; 20: 336-343.
[9] Pierro A and Eaton S. Intestinal ischemia reperfusion injury and multisystem organ failure. Semin Pediatr Surg 2004; 13: 11-17.
[10] Campolo M, Di Paola R, Impellizzeri D, Crupi R, Morittu VM, Procopio A, Perri E, Britti D, Peli A, Esposito E and Cuzzocrea S. Effects of a polyphenol present in olive oil, oleuropein aglycone, in a murine model of intestinal ischemia/reperfusion injury. J Leukoc Biol 2013; 93: 277-287.
[11] Lin SQ, Wei XH, Huang P, Liu YY, Zhao N, Li Q, Pan CS, Hu BH, Chang X, Fan JY, Yang XY, Wang CS, Liu HN and Han JY. QiShenYiQi Pills(R) prevent cardiac ischemia-reperfusion injury via energy modulation. Int J Cardiol 2013; 168: 967-974.
[12] Mallick IH, Yang W, Winslet MC and Seifalian AM. Ischemia-reperfusion injury of the intestine and protective strategies against injury. Dig Dis Sci 2004; 49: 1359-1377.
[13] Yasuhara H. Acute mesenteric ischemia: the challenge of gastroenterology. Surg Today 2005; 35: 185-195.
[14] Grootjans J, Lenaerts K, Derikx JP, Matthijsen RA, de Bruine AP, van Bijnen AA, van Dam RM, Dejong CH and Buurman WA. Human intestinal ischemia-reperfusion-induced inflammation characterized: experiences from a new translational model. Am J Pathol 2010; 176: 2283-2291.
[15] Liu KX, Li YS, Huang WQ, Chen SQ, Wang ZX, Liu JX and Xia Z. Immediate postconditioning during reperfusion attenuates intestinal injury. Intensive Care Med 2009; 35: 933-942.
[16] Gitter AH, Bendfeldt K, Schulzke JD and Fromm M. Leaks in the epithelial barrier caused by spontaneous and TNF-alpha-induced single-cell apoptosis. FASEB J 2000; 14: 1749-1753.
[17] Jiang J, Goel R, Iftekhar MA, Visaria R, Belcher JD, Vercellotti GM and Bischof JC. Tumor necrosis factor-alpha-induced accentuation in cryoinjury: mechanisms in vitro and in vivo. Mol Cancer Ther 2008; 7: 2547-2555.
[18] Lin HI, Chou SJ, Wang D, Feng NH, Feng E and Chen CF. Reperfusion liver injury induces down-regulation of eNOS and up-regulation of iNOS in lung tissues. Transplant Proc 2006; 38: 2203-2206.
[19] Liu WJ, Tang HT, Jia YT, Ma B, Fu JF, Wang Y, Lv KY and Xia ZF. Notoginsenoside R1 attenuates renal ischemia-reperfusion injury in rats. Shock 2010; 34: 314-320.
[20] Sun B, Xiao J, Sun XB and Wu Y. Notoginsenoside R1 attenuates cardiac dysfunction in endotoxemic mice: an insight into oestrogen receptor activation and PI3K/Akt signalling. Br J Pharmacol 2013; 168: 1758-1770.